ACCOUNTS
of chemical research

Synthesis and Selected Properties of Graphene and Graphene Mimics

C. N. R. RAO,* H. S. S. RAMAKRISHNA MATTE, AND K. S. SUBRAHMANYAM

Chemistry and Physics of Materials Unit, CSIR Centre of Excellence in Chemistry and International Centre for Materials Science, Jawaharlal Nehru Centre for Advanced Scientific Research, Jakkur P.O., Bangalore 560 064, India

RECEIVED ON JANUARY 29, 2012

CONSPECTUS

Graphene has generated great excitement in the last few years because of its novel properties with potential applications. Graphene exhibits an ambipolar electric field effect, ballistic conduction of charge carriers, and the quantum Hall effect at room temperature. Some of the other interesting characteristics of graphene include high transparency toward visible light, high elasticity and thermal conductivity, unusual magnetic properties, and charge transfer interactions with molecules.

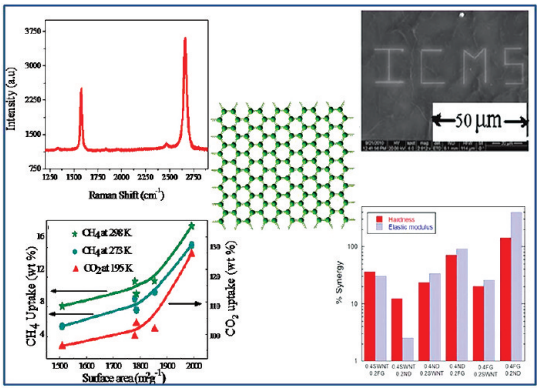

In this Account, we present the highlights of some of our research on the synthesis of graphene and its properties. Since the isolation and characterization of graphene by micromechanical cleavage from graphite, several strategies have been developed for the synthesis of graphene with either a single or just a few layers. The most significant contribution from our laboratory is the synthesis of two to four layer graphene by arc-discharge of graphite in a hydrogen atmosphere. Besides providing clean graphene surfaces, this method allows for doping with boron and nitrogen. UV and laser irradiation of graphene oxide provides fairly good graphene samples, and laser unzipping of nanotubes produces graphene nanoribbons. We have exploited Raman spectroscopy to investigate the charge-transfer interactions of graphene with electron-donor and -acceptor molecules, as well as with nanoparticles of noble metals. Graphene quenches the fluorescence of aromatics because of electron transfer or energy transfer.

Notable potential applications of the properties of graphene are low turn-on field emission and radiation detection. High-temperature ferromagnetism is another intriguing feature of graphene. Although incorporation of graphene improves the mechanical properties of polymers, its incorporation with nanodiamond or carbon nanotubes exhibits extraordinary synergy. The potential of graphene and its analogues as adsorbents and chemical storage materials for H_2 and CO_2 is noteworthy.

Introduction

Graphene has generated great excitement in the last few years owing to its novel properties with potential applications.[1] Graphene exhibits ambipolar electric field effect, ballistic conduction of charge carriers, and quantum Hall effect at room temperature.[2] Some of the other interesting aspects of graphene include high transparency toward visible light, high values of elasticity and thermal conductivity, unusual magnetic properties, and charge transfer interaction with molecules.[3,4] While graphene research is of recent origin, synthesis and modification of graphite-related materials have received the attention of chemistry for some decades.[4] Thus, early theoretical studies predicted some unusual electronic properties of graphene.[5] Procedures employed to generate single-layer graphene (SLG) in the early years were not successful.[6] It is only in 2004 that Novoselov et al.[1,2] successfully isolated single- and few-layer graphenes from highly oriented pyrolytic graphite (HOPG) by micromechanical cleavage and reported their unusual electronic characteristics. This technique has since been extended to other layered materials such as metal dichalcogenides.[7] In the past few years, several other strategies have been developed for the synthesis of graphene. A variety of microscopic and spectroscopic techniques have been

Published on the Web 06/27/2012 www.pubs.acs.org/accounts
10.1021/ar300033m © 2012 American Chemical Society

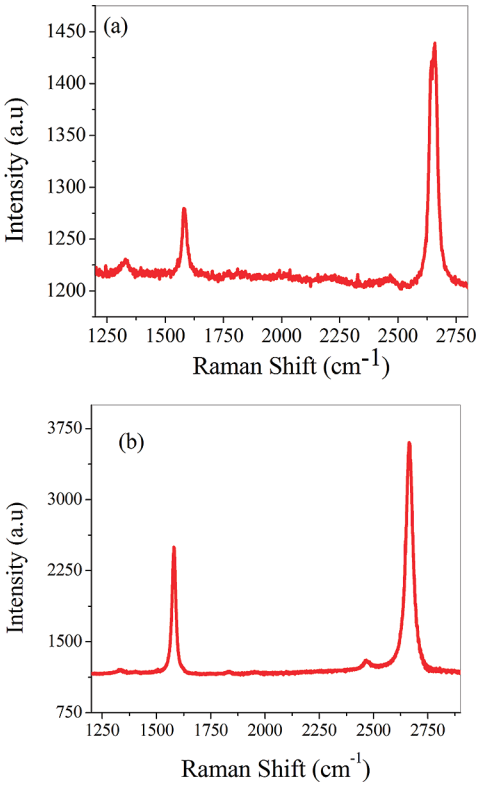

FIGURE 1. Raman spectra of graphene prepared by the thermal decomposition of (a) methane (70 sccm) and (b) benzene (argon passed through benzene with flow rate of 200 sccm) at 1000 °C on a nickel sheet. From ref 11.

employed to determine the purity and the number of layers in graphene samples.[8−10] Raman spectroscopy is an invaluable tool to characterize graphene in terms of both the number of layers and the electronic structure. We started research on graphene in 2006 and have since explored the synthesis and several of its properties. In this Account, we present the highlights of some of the results obtained by us on various aspects of graphene.

Synthesis

SLG has been synthesized by several methods such as epitaxial growth, chemical vapor deposition (CVD), solution phase exfoliation of graphite, and reduction of single-layer graphene oxide (SGO).[3] We have carried out CVD using various hydrocarbons on different metal catalysts[11] and found the growth of graphene films to depend on the hydrocarbon source and reaction conditions. On a nickel foil, CVD of methane (60−70 sccm) or ethylene (4−8 sccm) diluted with hydrogen (500 sccm) at 1000 °C for 5−10 min yielded SLG. In the case of benzene, vapors diluted with argon and hydrogen were decomposed at 1000 °C for 5 min. On a cobalt foil, acetylene (4 sccm) and methane (65 sccm)

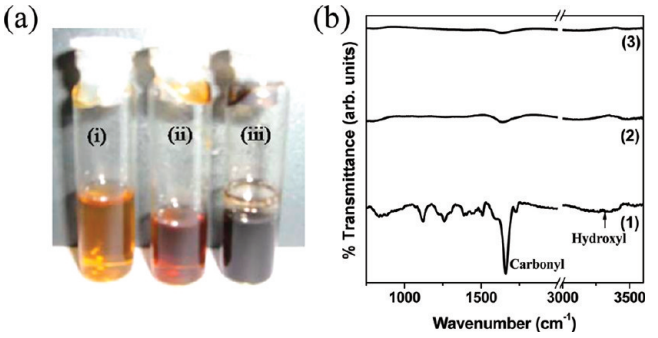

FIGURE 2. (a) Photographs of SGO (i) before and (ii) after irradiation with an excimer laser (300 mJ, 1000 shots) and (iii) after 18000 shots. (b) IR spectra of (1) SGO and SGO (2) after ultraviolet light exposure for 2 h and (3) after excimer laser treatment for 40 min. From ref 14.

diluted with hydrogen (500 sccm) were decomposed at 800 and 1000 °C, respectively. Figure 1 shows the Raman spectra of graphene sheets obtained by CVD on a nickel foil. The narrow line width (30−40 cm^{-1}) and relatively high intensity of the 2D band (~2670 cm^{-1}) indicate that these graphene samples predominantly contain single layers.[12]

A standard method employed for the synthesis of SLG involves the exfoliation of graphite oxide, followed by reduction.[13] The product obtained by this method is reduced graphene oxide (RGO), rather than graphene, since the surface of the graphene contains considerable oxygen functionalities. Reduction of SGO is generally carried out by using hydrazine hydrate as the reducing agent in dimethylformamide medium. We have found that microwave irradiation during reduction of SGO is effective, and it takes only 10 min for the reduction. RGO formed by this method has fewer defects as revealed by Raman spectroscopy. Oxygen functionalities in SGO can be minimized by irradiation with ultraviolet radiation or excimer laser.[14,15] In order to do so, a SGO solution is irradiated with a mercury lamp (254 nm, 25 W, 90 $\mu W/cm^2$). In the IR spectrum, bands due to carbonyl stretching and other oxygen-containing functional groups decrease in intensity markedly after ultraviolet irradiation for 2 h. Some changes are observed in the FESEM images, and more graphene edges become visible.[14,16] For laser irradiation, a KrF excimer laser (248 nm, 5 Hz) is generally employed. Figure 2a shows how the yellow colored solution of graphene oxide turns black on irradiation with the laser. Infrared spectra in Figure 2b show similar effects by irradiation with ultraviolet light (for ~2 h) and by excimer laser radiation (30−40 min). This technique has been usefully employed for patterning of graphene oxide (Figure 3a).[16] We have also carried out e-beam patterning of graphene oxide films to obtain patterns of RGO as thin as 250 nm

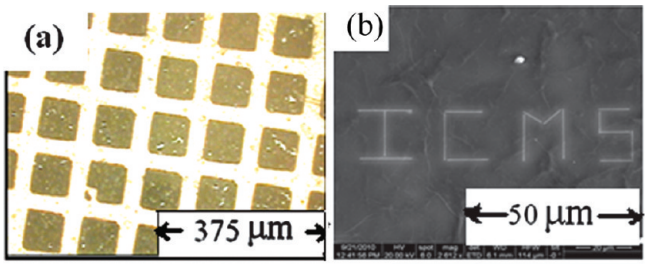

FIGURE 3. (a) Optical microscope image of the pattern achieved after excimer laser reduction of graphene oxide and (b) electron-beam pattern with 250 nm wide lines of RGO on GO films. From ref 16.

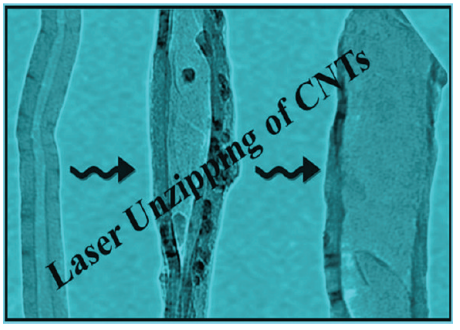

FIGURE 4. The process of unzipping of carbon nanotubes on irradiation with laser. From ref 17.

(Figure 3b). Prior to the irradiation, the material is insulating, and it becomes conducting after irradiation. Another important use of laser irradiation is to unzip carbon nanotubes to obtain graphene nanoribbons (GNRs).[17] Figure 4 shows the process of laser unzipping of carbon nanotubes.

The most common method to produce few-layer graphene is by exfoliation of graphite oxide at high temperatures.[18] We designate the few-layer graphene prepared by this procedure as exfoliated graphene (EG) and show typical TEM and AFM images in Figure 5a,b, respectively. Another approach to prepare few-layer graphene (DG) is thermal conversion of nanodiamond in the temperature range of 1650−2200 °C in helium atmosphere.[11,18,19] We have developed a method to prepare graphene samples with 2−4 layers by carrying out arc-evaporation of graphite in a hydrogen atmosphere (HG).[20] The presence of hydrogen during the arc-discharge process terminates the dangling carbon bonds preventing the formation of closed structures. In a typical experiment, a graphite rod (6 mm in diameter and 50 mm long) was used as the anode, and another graphite rod (13 mm in diameter and 60 mm in length) was used as the cathode. Figure 5c,d shows TEM and AFM images, respectively, of graphene sheets with two to three layers.

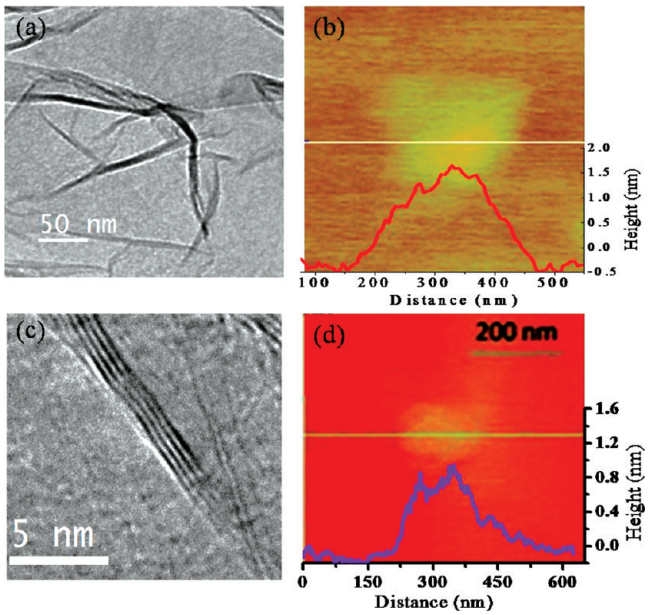

FIGURE 5. TEM images of (a) EG and (c) HG and AFM images of (b) EG and (d) HG. From ref 22.

Surface Area and Gas Adsorption

Brunauer−Emmet−Teller (BET) surface areas of few-layer graphenes are in the range of 270−1550 m^2/g, with the trend EG > DG > RGO > HG.[21,22] In Figure 6a, we show the N_2 adsorption data of EG with a surface area of 1250 m^2/g at 77 K. Uptake of CO_2 by graphene samples varies between 5 and 45 wt % (at 195 K and 1 atm), with EG exhibiting the highest uptake. The uptake of CO_2 by EG at 298 K and 50 bar is 51 wt %.[22] In Figure 6b, we show typical CO_2 adsorption data of an EG sample at 195 K, 1 atm. H_2 adsorption measurements show that EG, DG, and HG absorb 1.7, 1.2, and 1.0 wt % of H_2 at 1 atm and 77 K and 3.1, 2.5, and 2.0 wt % at at 100 bar and 300 K. The uptake of CH_4 by graphene samples varies between 0 and 3 wt %, EG showing the highest value.[22]

Charge-Transfer Interaction with Donor and Acceptor Molecules

Being an extended π-system, graphene exhibits charge-transfer interactions with electron-donor and electron-acceptor molecules. This aspect has been studied in detail by us by employing Raman spectroscopy and calorimetric experiments.[23−26] On interaction with electron-donor molecules such as tetrathiafulvalene (TTF), the Raman G-band softens progressively with the increase in concentration while the band stiffens with increasing concentration of electron-withdrawing molecules such as tetracyanoethylene (TCNE) (Figure 7a). The full-width at half-maximum (fwhm) of the G-band increases (Figure 7b) and the intensity

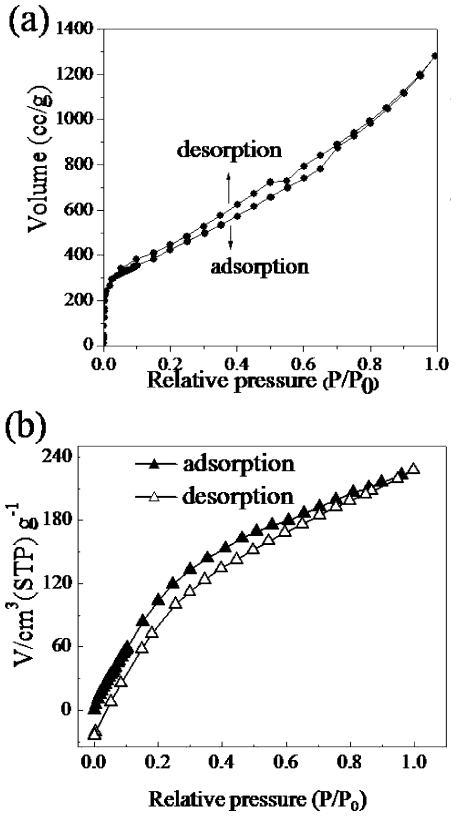

FIGURE 6. (a) Nitrogen and (b) carbon dioxide adsorption and desorption isotherms of EG. From ref 22.

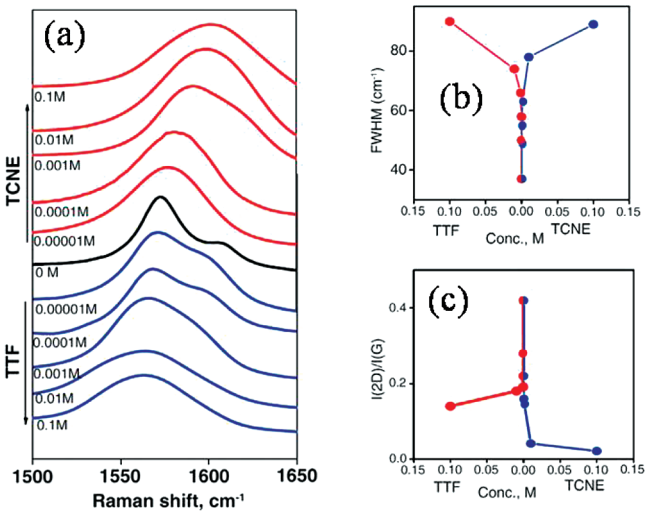

FIGURE 7. Variation in (a) position and (b) fwhm of Raman G-band and (c) I_{2D}/I_G intensity ratio of graphene with the concentrations of TTF and TCNE. From ref 25.

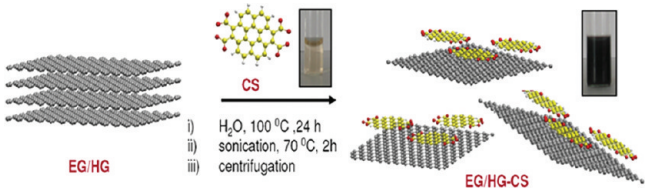

FIGURE 8. Illustration of the exfoliation of few-layer graphene with CS to yield monolayer graphene–CS composites. From ref 30.

of the 2D-band decreases markedly on interaction with these molecules. The ratio of intensities of the 2D and G bands, I_{2D}/I_G, is a sensitive probe to examine the effect of the electron-donor and -acceptor molecules on the electronic structure of graphene. The I_{2D}/I_G ratio decreases markedly with the concentration of both electron-donor and electron-acceptor molecules (Figure 7c). Electronic absorption spectra also provide the evidence of molecular charge transfer. The shifts in the G-band caused by molecular charge transfer differ from those due to electrochemical doping where the G-band increases in frequency for both the electron and hole doping.[27,28] Isothermal titration calorimetry (ITC) experiments show that interaction energies of the graphene with electron-acceptor molecules are higher than those with electron-donor molecules and increase progressively with the electron affinities of the acceptors.[26] DFT calculations show that interaction with molecules such as TCNE open a gap in graphene. The magnitude of interaction between graphene and donor/acceptor molecules is dependent on the surface area of the graphene.[29] Charge transfer of graphene with coronene tetracarboxylate (CS) has been exploited for solubilization and exfoliation (Figure 8).[30] Such charge-transfer also provides the basis for sensor properties of graphene for gases like NO_2.[31]

Decoration with Metal Nanoparticles

Decoration of graphene with metal nanoparticles causes changes in the electronic structure of graphene through Columbic charge transfer. Such hybrid materials may be of use in catalysis, nanoelectronics, optics, and nanobiotechnology.[32−35] We have employed a simple, green approach for the decoration of noble metal nanoparticles on the graphene surface, using ethylene glycol as the solvent and reducing agent in a domestic microwave oven. On interaction with nanoparticles of metals such as Ag, Au, Pt, and Pd, the Raman G-band shifts to higher frequencies, accompanied by a variation in the relative intensities of D and 2D bands.[36] The magnitude of the G-band shift decreases with increase in ionization energy (Au > Pt > Pd > Ag) of the metal. In addition, nanoparticles of ZnO and TiO_2, as well as magnetic nanoparticles of oxides such as Fe_3O_4 and $CoFe_2O_4$, interact with graphene giving rise to changes in the Raman spectra and magnetic properties.[37]

Quenching of Fluorescence of Aromatics

Graphene possesses many interesting optical properties. One of them is the blue emission exhibited by RGO and other oxidized graphene samples.[38] White light has been

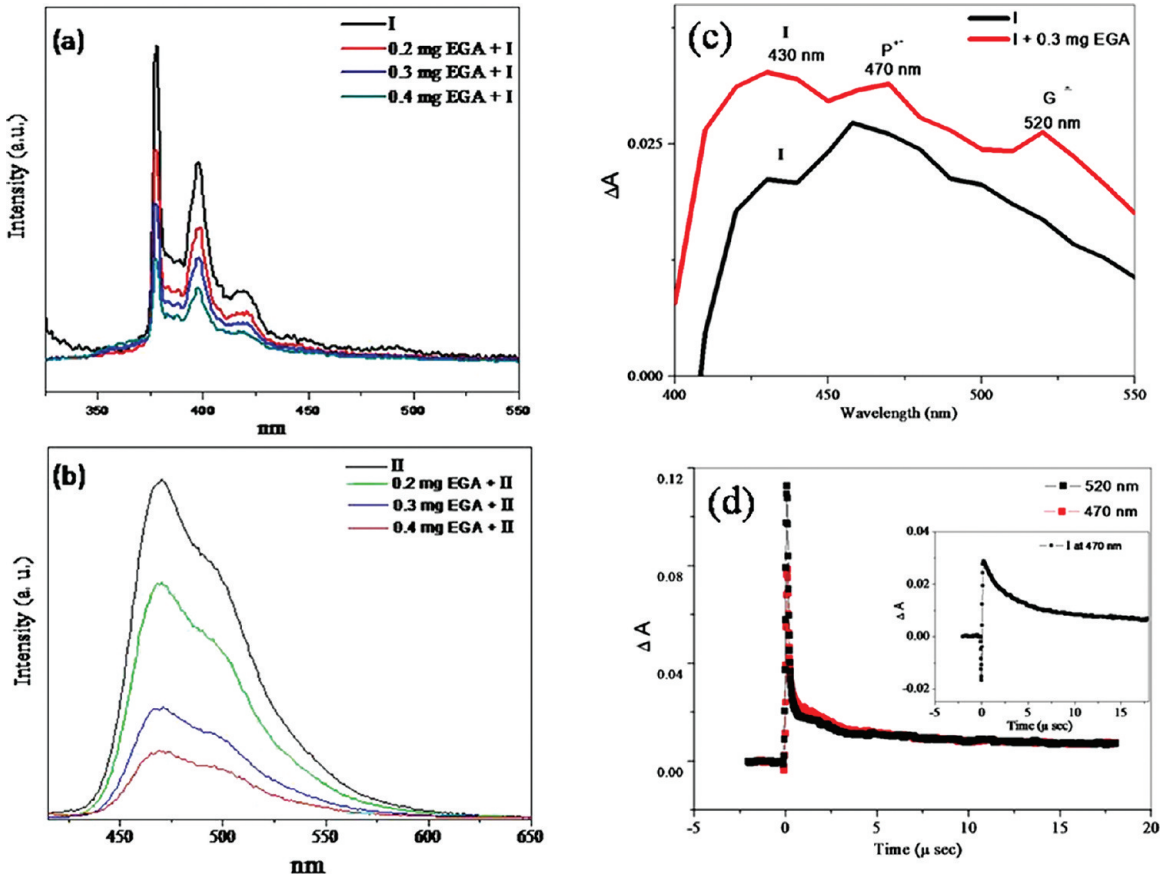

FIGURE 9. Fluorescence spectra of (a) PyBS (I, 10^{-5} M in DMF) and (b) OPV ester (II, 10^{-5} M in chloroform) with increasing concentrations of graphene (EGA). (c) Effect of addition of EGA on the transient absorption spectrum of PyBS, (I, λ_{exc}=355 nm) after 500 ns and (d) lifetime decay of transient species of PyBS + EGA recorded at 470 and 520 nm. Inset shows the decay of pure PyBS at 470 nm. From ref 39.

produced in combination with a yellow emitter. Interaction with amide-functionalized graphene (EGA) with the electron donors, pyrene-butanaoic acid succinimidyl ester (PyBS, I) and oligo(*p*-phenylene vinylene) methyl ester (OPV-ester, II), causes a marked decrease in the intensity of the fluorescence bands of the donors as illustrated in Figure 9a,b.[39] Transient absorption measurements show a broad band in the 450−530 nm range due to the triplet state and new bands around 470 and 520 nm in the transient absorption spectrum at 500 ns (Figure 9c) due to the pyrenyl radical cation and the graphene radical anion, respectively. The decay of the radical cation is fast as evidenced from the appearance of a short-lived component (900 ns) in the decay profile (Figure 9d). Kamat et al.[40] invoke electron transfer to explain interaction of porphyrin with graphene. Preliminary results show that electron acceptor molecules are likely to interact with graphene via energy transfer.

Doping with Nitrogen and Boron

Efforts have been made to dope graphene with boron and nitrogen.[41−43] In order to dope graphene without affecting its surface, the arc-evaporation technique is useful.[43] To dope with boron, arc discharge of graphite is carried out in the presence of H_2 + diborane or by using boron-stuffed carbon electrodes. Doping with nitrogen is accomplished by carrying out discharge in an atmosphere of NH_3 or pyridine + H_2 mixture. The Raman G-band shifts to higher frequencies in comparison with pristine samples on B and N doping just as in the case of electrochemical doping.[26] In Figure 10, we show the shifts of the G-band caused by nitrogen and boron doping. The ratio of intensities of the D and G bands, $I_{(D)}/I_{(G)}$, increases where as the ratio of intensities of the 2D and G bands, $I_{(2D)}/I_{(G)}$, decreases in the doped samples. N- and B-doped graphenes show different photodegradation kinetics with rhodamine 6G and methylene blue.[44]

Chemical Storage of Hydrogen and Halogens

Since the uptake of hydrogen by graphene samples by adsorption does not exceed ~3 wt %, we have examined chemical storage of hydrogen through hydrogenation. Hydrogenation of graphene by cold hydrogen plasma and

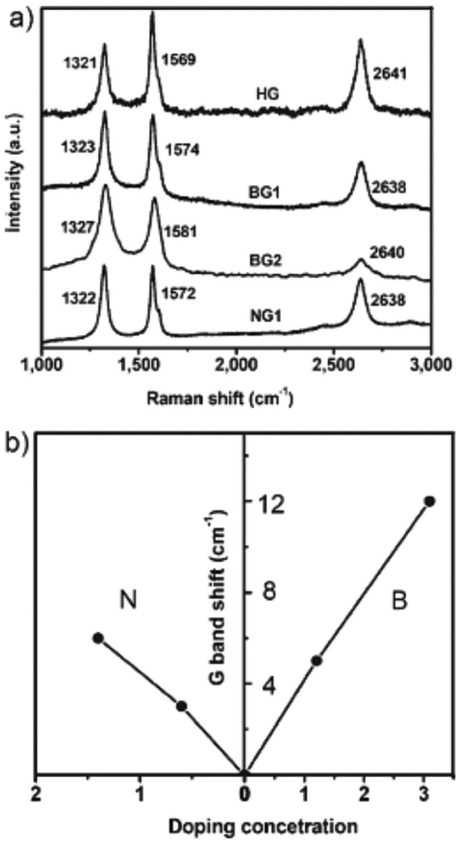

FIGURE 10. (a) Raman Spectra of undoped (HG) and doped (BG and NG) graphene samples. (b) Shifts of the G-band caused by electron (N) doping and hole (B) doping. From ref 43.

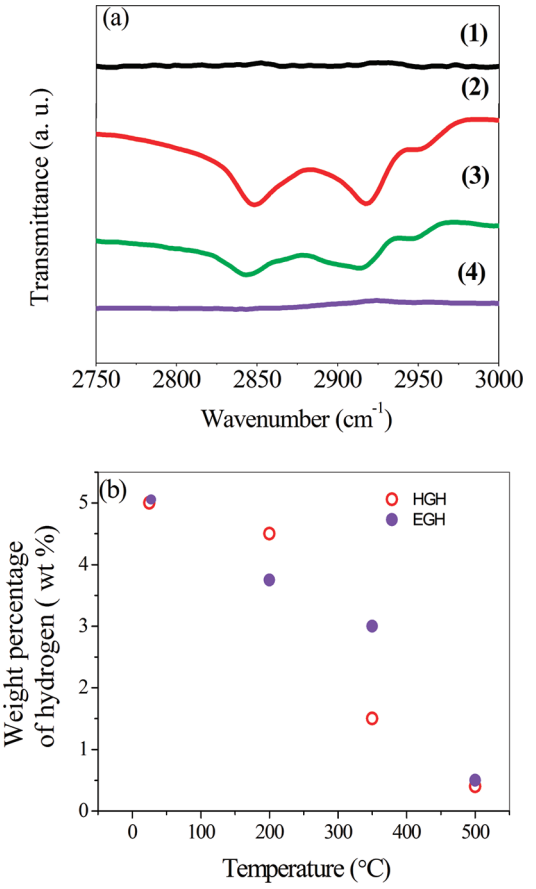

FIGURE 11. (a) IR spectra of (1) EG, (2) EGH, and EGH heated for 4 h (3) at 200 °C and (4) at 500 °C. (b) Change in hydrogen content of EGH and HGH with temperature. From ref 47.

by using radio frequency catalytic CVD has been reported.[45,46] We have also carried out the plasma hydrogenation of graphene but only obtained a hydrogen content of up to 1.8 wt %. We have, therefore, carried out hydrogenation of various graphene samples by Birch reduction.[47] Infrared (IR) spectra of the hydrogenated samples (EGH, HGH) show aliphatic C−H stretching bands (Figure 11a), and elemental analysis revealed the hydrogen content to be around 5 wt % (maximum possible value is ~7.7 wt %). Birch reduction of graphene nanoribbons (GNR) prepared by oxidative unzipping of carbon nanotubes showed a H_2 uptake of 3 wt %. The hydrogenated samples were stable at room temperature and get dehydrogenated on annealing at 500 °C (Figure 11b). Dehydrogenation could also be carried out by UV or excimer laser irradiation. This transformation can be exploited for patterning.[16]

Chlorination of graphene by irradiation with UV light in liquid chlorine yields up to 56 wt % chlorine in the sample.[48] Interestingly, chlorination too is reversible. Reversible bromination of graphene up to 25 wt % has also been achieved.

Magnetic Properties

Room-temperature ferromagnetism in graphene and graphite-based materials has attracted considerable interest. Yazyev and Helm[49] showed that magnetism in graphene can be induced by defects. Zig-zag edges have been considered to be responsible for the magnetism of graphene by many workers.[50] Wang et al.[51] reported room-temperature ferromagnetism in a graphene sample prepared by reduction of graphene oxide. We have measured the magnetic properties of a variety of graphene samples.[52,53] All the samples show divergence between the field-cooled (FC) and zero-field-cooled (ZFC) data, starting around 300 K (Figure 12a). The divergence nearly disappears on application of 1 T. Temperature-dependent magnetization data of graphenes are comparable to those of magnetically frustrated systems, wherein different types of magnetic states coexist. The graphene samples show magnetic hysteresis at room temperature (Figure 12b) and the saturation magnetization (M_S) increases with decrease in temperature, the value being highest in the case of HG. EPR measurements in the

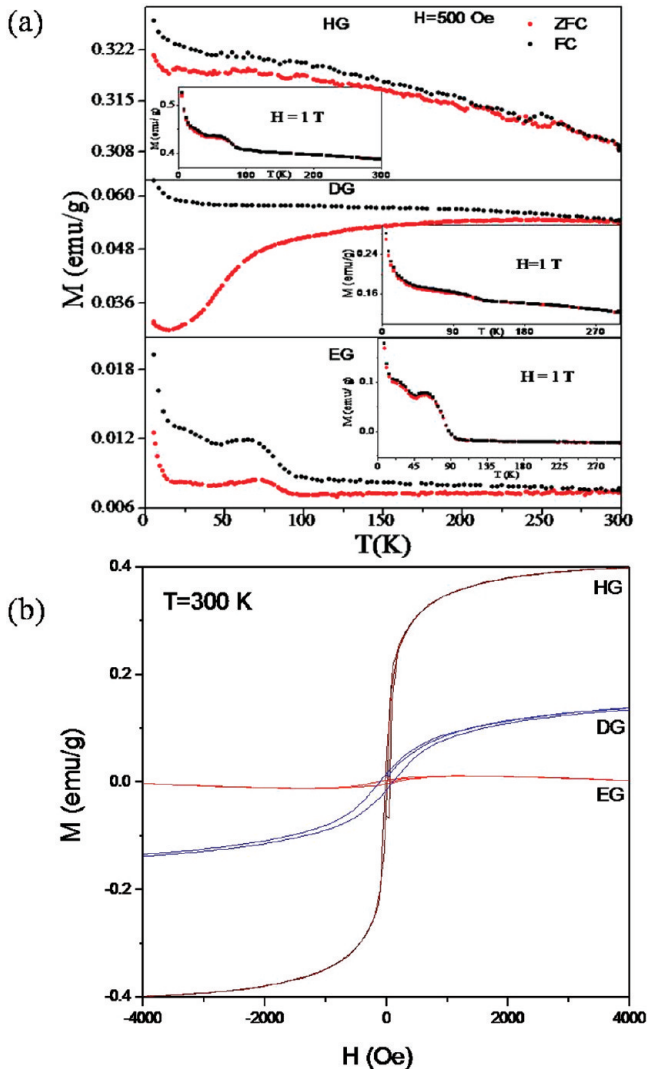

FIGURE 12. (a) Temperature variation of magnetization of EG, DG, and HG at 500 Oe. (Inset shows data at 1 T). (b) Magnetic hysteresis in EG, DG, and HG at 300 K. Reproduced from ref 52. Copyright 2009 American Chemical Society.

2.5−300 K range show a signal with a line width of 0.7−2.9 mT and a *g*-value in the 2.006−2.013 range, suggesting that spins do not originate from transition-metal impurities but from the spin species in the graphenes.

Adsorption of the benzene solutions of tetrathiafulvalane (TTF) and tetracyanoethylene (TCNE) on graphene decreases the magnetization value while still showing room-temperature hysteresis.[52,53] Hydrogenated graphenes show an increase in the magnetic moment with increase in the hydrogen content. On dehydrogenation at 500 °C for 4 h, the samples exhibit a decrease in the magnetic moment.[53]

Field-Emission Properties

Graphene films prepared by electrophoretic deposition have been demonstrated to show good field-emission properties

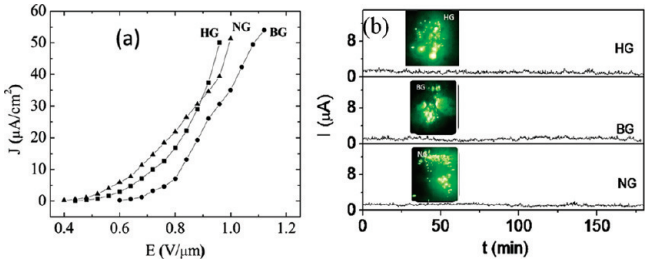

FIGURE 13. (a) Current density (*J*) of HG, BG, and NG as a function of electric field. (b) Current stability of HG, BG, and NG (Inset shows field emission pattern corresponding to HG, BG, and NG). From ref 55.

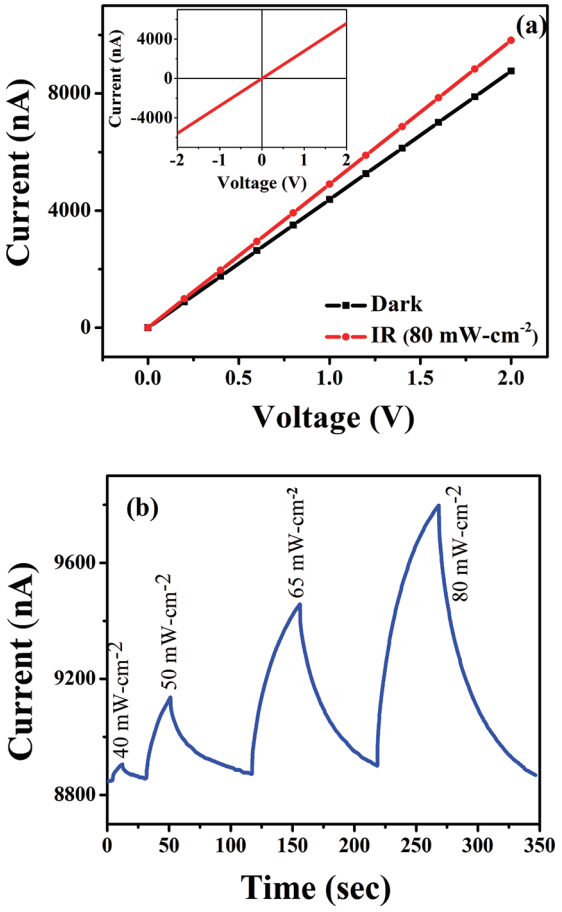

FIGURE 14. (a) Typical *I*−*V* characteristics of RGO in the dark and under illumination at 1550 nm at 80 mW cm^{-2}. The inset shows metal−RGO−metal contact. (b) Photocurrent as a function of time with different IR intensities at 2 V for RGO. From ref 59.

with a low turn-on electric field (E_{to} = 2.3 V μm^{-1} at 10 μA cm^{-2}), a large field-enhancement factor (3000), and good emission stability, better than those of CNTs.[54] In Figure 13a, we show the variation in current density (*J*) of the HG, as well as boron and nitrogen doped HG, samples (BG and NG, respectively) with electric field (*E*).[55] The turn-on electric field (at 10 μA cm^{-2}) is 0.7, 0.8, and 0.6 V μm^{-1} for HG, BG, and NG, respectively. The low turn-on electric field[56] for NG

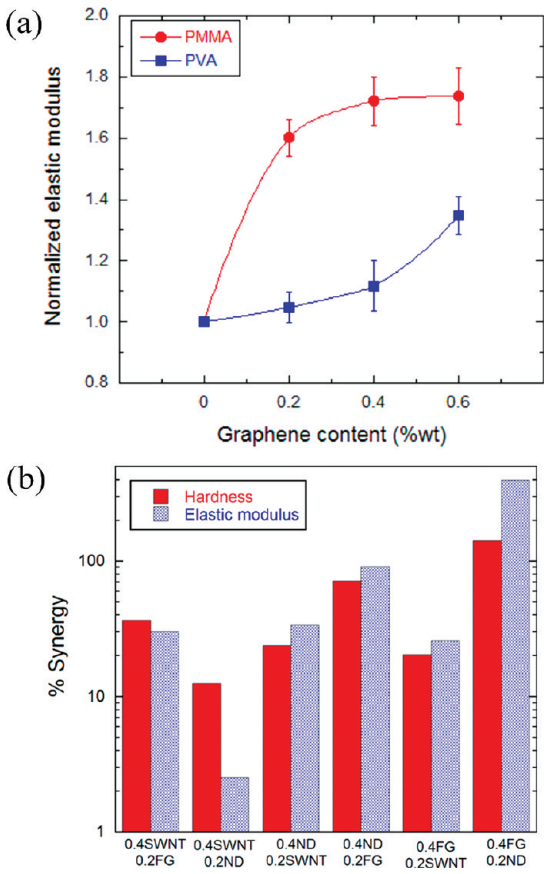

FIGURE 15. (a) Normalized elastic modulus plotted with graphene content for PVA and PMMA composites. (b) Percentage synergy in hardness and elastic modulus for different binary composites. From ref 63.

might be due to the upshift of Fermi level of graphene. The emission currents are stable over a period of more than 3 h (Figure 13b), revealing that the field-emission characteristics of the graphene samples are superior to many other nanomaterials.

Photodetectors

Graphene FETs have been studied widely. Our own studies have shown that FETs fabricated from RGO exhibit ambipolar characteristics.[57] N- and B-doped graphenes show n-type and p-type transfer characteristics, respectively. Graphene also exhibits good infrared (IR) detection properties.[58] We have fabricated IR detectors of graphene prepared by chemical methods.[59] Electrical conductivities of RGO and graphene nanoribbons (GNRs) increase with IR laser radiation and can even sense the IR radiation emitted from a human body. In Figure 14, we show the change in $I-V$ characteristics of RGO with the illumination of IR radiation (1550 nm at 80 mW cm $^{-2}$) and the effect of intensity of IR radiation. The inset in the Figure 14a shows metal–RGO–metal contact. The current

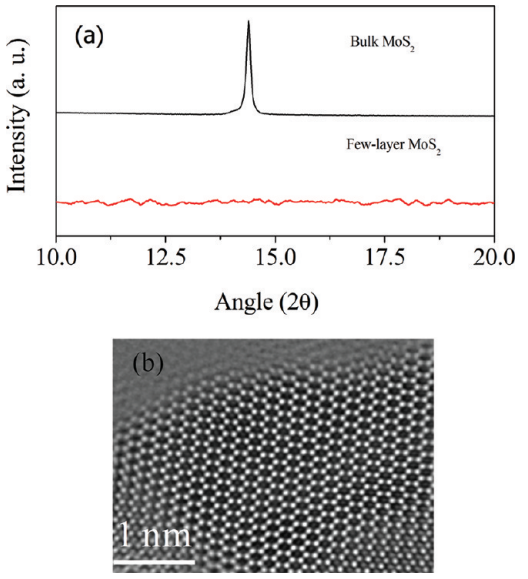

FIGURE 16. (a) XRD patterns of bulk MoS_2 and few-layered MoS_2. (b) High-resolution TEM image of $MoSe_2$. From refs 66 and 67.

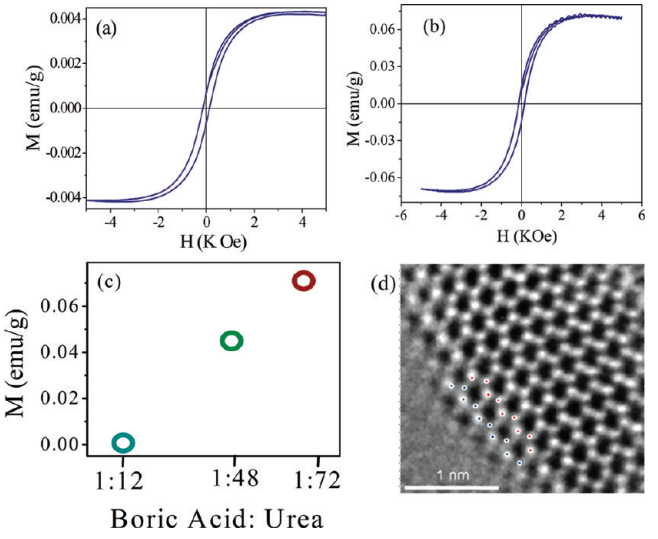

FIGURE 17. Magnetic hysteresis exhibited by graphene-like (a) MoS_2 and (b) BN at 300 K. (c) shows layer dependence of magnetism of BN. (d) High-resolution TEM image showing zigzag edges in graphene-like MoS_2. From ref 53.

responsivity (R_λ) and the external quantum efficiency (EQE) for RGO is 4 mA/W and 0.3%, respectively, while for GNR these values are higher, being 1 A/W and 80%, respectively, for an incident wavelength of 1550 nm at 2 V. Graphene is also a good UV absorber.[60] UV-detectors based on RGO show a responsivity of 0.12 A/W with an EQE of 40%.[61]

Mechanical Properties

Ramanathan et al.[62] reported that incorporation of ~1 wt % of functionalized graphene in a poly(methyl methacrylate)

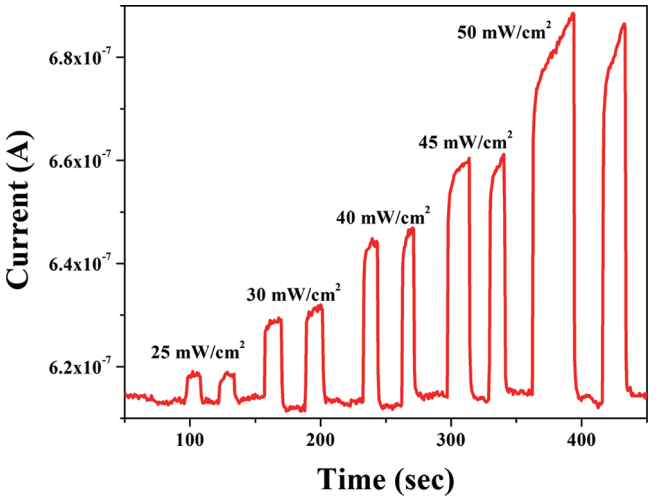

FIGURE 18. Photocurrent as a function of time with different IR intensities at 0.1 V for few-layer $MoSe_2$. From ref 69.

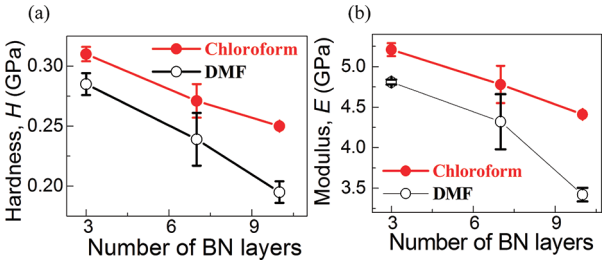

FIGURE 19. Variation of (a) hardness and (b) elastic modulus of BN–PMMA composites prepared in chloroform and dimethylformamide (DMF) as a function of number of BN layers. From ref 70.

(PMMA) matrix causes an increase of 80% in elastic modulus and 20% in ultimate tensile strength. We have investigated the performance of functionalized EG as a filler material in poly(vinyl alcohol) (PVA) and PMMA matrices by employing the nanoindentation technique. The addition of 0.6 wt % of EG results a significant increase in both the elastic modulus and hardness (Figure 15a). The observed improvement in the mechanical properties of the polymers is attributed to the interaction between the polymer and graphene, which in turn provides better load-transfer between the matrix and the fiber. We have studied the effect of binary combinations of nanodiamond (ND), few-layer graphene (EG), and single-walled nanotubes (SWNT) as fillers in PVA matrices.[63] There is an extraordinary synergy with improvement by as much as 400% in stiffness and hardness compared with those obtained with single nanocarbon reinforcements. The synergistic effect was dramatic in the case of ND–EG composite with 4- and 1.5-fold increases in elastic modulus and hardness, respectively (Figure 15b).

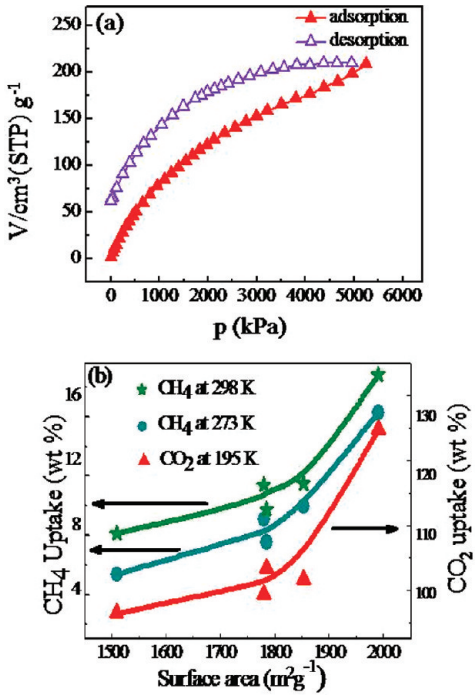

FIGURE 20. (a) CH_4 uptake curves of BCN at 298 K and 50 bar. (b) Plot of the BET surface area and the weight percentage of methane uptake (at 50 bar of pressure, 273 and 298 K) and carbon dioxide uptake (at 1 bar and 195 K) of BCN. From ref 22.

Graphene Mimics

Inorganic analogues of zero-dimensional fullerenes and one-dimensional carbon nanotubes formed by various layered materials have been prepared and characterized.[64] There have been efforts to prepare graphene-like MoS_2, BN, and other layered materials. Single- and few-layer materials of these have been prepared by micromechanical cleavage or ultrasonication of dispersions in liquids.[65] Chemical methods have been successfully applied for generating these graphene analogues. In the case of MoS_2, WS_2, $MoSe_2$, and WSe_2, intercalation of the bulk material with lithium followed by sonication in water, reaction of molybdic or tungstic acid with excess thiourea or selenourea at 773 K in a nitrogen atmosphere, or reaction of KSCN or Se with H_2MoO_4 under hydrothermal conditions have been employed.[66,67] The XRD patterns provide evidence for the formation of the graphene analogues, through the absence of the (002) reflection (Figure 16a) while the Raman spectra show shifts and broadening of the bands due to the A_{1g} and E_{2g} modes. In Figure 16b, we show a high-resolution TEM image of $MoSe_2$. We have prepared BN sheets by the reaction of boric acid and urea at high temperatures.[68]

Graphene analogues of MoS_2, WS_2, $MoSe_2$, WSe_2, and BN exhibit room-temperature ferromagnetism due to edge

effects (Figure 17a,b). There is an increase in the magnetic moment with the decreasing number of layers (see Figure 17c). We show the presence of edges in graphene-like MoS_2 in Figure 17d. Few-layer MoS_2 and $MoSe_2$ exhibit good IR radiation detection properties. The responsivity and EQE of the $MoSe_2$ device are specially good (Figure 18), the values being 50 mA/W and 6%, respectively, at an incident wavelength of 1064 nm.[69] Mechanical properties of PMMA–BN composites with different numbers of BN layers show that the composite with the least number of BN layers has the highest hardness and elastic modulus (Figure 19).[70]

Besides graphene analogues of known materials, it is of value to generate new graphene-like materials. One success in this direction is the synthesis of high-surface area $B_xC_yN_z$ containing a few layers, with an average composition between BCN and BC_2N, prepared by the reaction of activated charcoal, boric acid, and urea.[22] They exhibit high uptake of both CO_2 and CH_4, the highest value of CO_2 uptake being 128 wt % at 195 K and 1 atm and 64% at room temperature and 50 bar pressure. The CH_4 uptake value varies from 7.5 to 17 wt % at 273 K. At 298 K, the highest uptake is 15 wt % (see Figure 20).

Conclusions

Our research on graphene has been exciting and rewarding. Some of the properties such as the synergy in mechanical properties of polymer composites found when graphene is incorporated along with another nanocarbon and the radiation detection characteristics are impressive. It is possible that graphene can be employed in flatbed displays due to the favorable field-emission characteristics. Possible use of graphene in organic photovoltaics is suggested by its excited-state interactions with fluorescent molecules. An early study in this laboratory indicated the possible use of graphene in supercapacitors.[71] Recent studies have indeed shown this to be a potential application. Graphene has also been used in lithium ion batteries and other energy related devices. While the 5 wt % reversible storage of hydrogen in graphene could possibly be useful in energy-related applications, the remarkable adsorptive properties of graphene-like BCN for CO_2 and CH_4 should certainly be explored for further use. Properties and applications of inorganic graphene mimics are worthy of exploration.

BIOGRAPHICAL INFORMATION

C. N. R. Rao obtained his Ph.D. degree from Purdue University (1958) and D.Sc. degree from the University of Mysore (1961). He is the National Research Professor and Linus Pauling Research Professor at the Jawaharlal Nehru Centre for Advanced Scientific Research (JNCASR) and honorary professor at the Indian Institute of Science (both at Bangalore). His research interests are mainly in the chemistry of materials. He is a member of many of the science academies and is the recipient of the Hughes and Royal Medals of the Royal Society, the August Wilhelm von Hofmann medal of the German Chemical Society, and the Dan David Prize for materials research.

H. S. S. Ramakrishna Matte obtained his M.S. degree in chemical science in 2009 from JNCASR and is pursuing Ph.D. studies.

K. S. Subrahmanyam received his M.S. (Engg) and Ph.D. degrees from JNCASR in 2008 and 2012, respectively.

FOOTNOTES

*Corresponding author. Fax: 00 91 80 2208 2766. E-mail: cnrrao@jncasr.ac.in.
The authors declare no competing financial interest.

REFERENCES

1 Novoselov, K. S.; Geim, A. K.; Morozov, S. V.; Jiang, D.; Zhang, Y.; Dubonos, S. V.; Grigorieva, I. V.; Firsov, A. A. Electric Field Effect in Atomically Thin Carbon Films. *Science* **2004**, *306*, 666–669.

2 Geim, A. K.; Novoselov, K. S. The Rise of Graphene. *Nat. Mater.* **2007**, *6*, 183–191.

3 Rao, C. N. R.; Sood, A. K.; Subrahmanyam, K. S.; Govindaraj, A. Graphene: The New Two-Dimensional Nanomaterial. *Angew. Chem., Int. Ed.* **2009**, *48*, 7752–7777.

4 Pati, S. K., Enoki, T., Rao, C. N. R., Eds. *Graphene and Its Fascinating Attributes*; World Scientific: Singapore, 2011.

5 Wallace, P. R. The Band Theory of Graphite. *Phys. Rev.* **1947**, *71*, 622–634.

6 Dreyer, D. R.; Ruoff, R. S.; Bielawski, C. W. From Conception to Realization: An Historial Account of Graphene and Some Perspectives for Its Future. *Angew. Chem., Int. Ed.* **2010**, *49*, 9336–9344.

7 Novoselov, K. S.; Jiang, D.; Schedin, F.; Booth, T. J.; Khotkevich, V. V.; Morozov, S. V.; Geim, A. K. Two-Dimensional Atomic Crystals. *Proc. Natl. Acad. Sci. U.S.A.* **2005**, *102*, 10451–10453.

8 Abergel, D. S.; Russell, A.; Falko, V. I. Visibility of Graphene Flakes on a Dielectric Substrate. *Appl. Phys. Lett.* **2007**, *91*, No. 063125.

9 Meyer, J. C.; Kisielowski, C.; Erni, R.; Rossell, M. D.; Crommie, M. F.; Zettl, A. Direct Imaging of Lattice Atoms and Topological Defects in Graphene Membranes. *Nano Lett.* **2008**, *8*, 3582–3586.

10 Hernandez, Y.; Nicolosi, V.; Lotya, M.; Blighe, F. M.; Sun, Z.; De, S.; McGovern, I. T.; Holland, B.; Byrne, M.; Gun'Ko, Y. K.; Boland, J. J.; Niraj, P.; Duesberg, G.; Krishnamurthy, S.; Goodhue, R.; Hutchison, J.; Scardaci, V.; Ferrari, A. C.; Coleman, J. N. High-Yield Production of Graphene by Liquid-Phase Exfoliation of Graphite. *Nat. Nanotechnol.* **2008**, *3*, 563–568.

11 Rao, C. N. R.; Subrahmanyam, K. S.; Matte, H. S. S. R.; Abdulhakeem, B.; Govindaraj, A.; Das, B.; Kumar, P.; Ghosh, A.; Late, D. J. A Study of the Synthetic Methods and Properties of Graphenes. *Sci. Technol. Adv. Mater.* **2010**, *11*, No. 054502.

12 Reina, A.; Jia, X. T.; Ho, J.; Nezich, D.; Son, H. B.; Bulovic, V.; Dresselhaus, M. S.; Kong, J. Large Area, Few-Layer Graphene Films on Arbitrary Substrates by Chemical Vapor Deposition. *Nano Lett.* **2009**, *9*, 30–35.

13 Dreyer, D. R.; Park, S.; Bielawski, C. W.; Ruoff, R. S. The Chemistry of Graphene Oxide. *Chem. Soc. Rev.* **2010**, *39*, 228–240.

14 Kumar, P.; Subrahmanyam, K. S.; Rao, C. N. R. Graphene Produced by Radiation-Induced Reduction of Graphene Oxide. *Int. J. Nanosci.* **2011**, *10*, 559–566.

15 Abdelsayed, V.; Moussa, S.; Hassan, H. M.; Aluri, H. S.; Collinson, M. M.; El-Shall, M. S. Photothermal Deoxygenation of Graphite Oxide with Laser Excitation in Solution and Graphene-Aided Increase in Water Temperature. *J. Phys. Chem. Lett.* **2010**, *1*, 2804–2809.

16 Kumar, P.; Subrahmanyam, K. S.; Rao, C. N. R. Graphene Patterning and Lithography Employing Laser/Electron-Beam Reduced Graphene Oxide and Hydrogenated Graphene. *Mater. Express* **2011**, *1*, 252–256.

17 Kumar, P.; Panchakarla, L. S.; Rao, C. N. R. Laser-Induced Unzipping of Carbon Nanotubes to Yield Graphene Nanoribbons. *Nanoscale* **2011**, *3*, 2127–2129.

18 Subrahmanyam, K. S.; Vivekchand, S. R. C.; Govindaraj, A.; Rao, C. N. R. A Study of Graphenes Prepared by Different Methods: Characterization, Properties and Solubilization. *J. Mater. Chem.* **2008**, *18*, 1517–1523.

19 Prasad, B. L. V.; Sato, H.; Enoki, T.; Hishiyama, Y.; Kaburagi, Y.; Rao, A. M.; Eklund, P. C.; Oshida, K.; Endo, M. Heat-Treatment Effect on the Nanosized Graphite Pi-Electron System during Diamond to Graphite Conversion. *Phys. Rev. B* **2000**, *62*, 11209–11218.

20 Subrahmanyam, K. S.; Panchakarla, L. S.; Govindaraj, A.; Rao, C. N. R. Simple Method of Preparing Graphene Flakes by an Arc-Discharge Method. *J. Phys. Chem. C* **2009**, *113*, 4257–4259.

21 Ghosh, A.; Subrahmanyam, K. S.; Krishna, K. S.; Datta, S.; Govindaraj, A.; Pati, S. K.; Rao, C. N. R. Uptake of H_2 and CO_2 by Graphene. *J. Phys. Chem. C* **2008**, *112*, 15704–15707.

22 Kumar, N.; Subrahmanyam, K. S.; Chaturbedy, P.; Raidongia, K.; Govindaraj, A.; Hembram, K. P. S. S.; Mishra, A. K.; Waghmare, U. V.; Rao, C. N. R. Remarkable Uptake of CO_2 and CH_4 by Graphene-Like Borocarbonitrides, BxCyNz. *ChemSusChem* **2011**, *4*, 1662–1670.

23 Das, B.; Voggu, R.; Rout, C. S.; Rao, C. N. R. Changes in the Electronic Structure and Properties of Graphene Induced by Molecular Charge-Transfer. *Chem. Commun.* **2008**, 5155–5157.

24 Voggu, R.; Das, B.; Rout, C. S.; Rao, C. N. R. Effects of Charge Transfer Interaction of Graphene with Electron Donor and Acceptor Molecules Examined Using Raman Spectroscopy and Cognate Techniques. *J. Phys.: Condens. Matter* **2008**, *20*, No. 472204.

25 Rao, C. N. R.; Voggu, R. Charge-Transfer with Graphene and Nanotubes. *Mater. Today* **2010**, *13*, 34–40.

26 Varghese, N.; Ghosh, A.; Voggu, R.; Ghosh, S.; Rao, C. N. R. Selectivity in the Interaction of Electron Donor and Acceptor Molecules with Graphene and Single-Walled Carbon Nanotubes. *J. Phys. Chem. C* **2009**, *113*, 16855–16859.

27 Das, A.; Pisana, S.; Chakraborty, B.; Piscanec, S.; Saha, S. K.; Waghmare, U. V.; Novoselov, K. S.; Krishnamurthy, H. R.; Geim, A. K.; Ferrari, A. C.; Sood, A. K. Monitoring Dopants by Raman Scattering in an Electrochemically Top-Gated Graphene Transistor. *Nat. Nanotechnol.* **2008**, *3*, 210–215.

28 Manna, A. K.; Pati, S. K. Tuning the Electronic Structure of Graphene by Molecular Charge Transfer: A Computational Study. *Chem.—Asian J.* **2009**, *4*, 855–860.

29 Subrahmanyam, K. S.; Voggu, R.; Govindaraj, A.; Rao, C. N. R. A Comparative Raman Study of the Interaction of Electron Donor and Acceptor Molecules with Graphene Prepared by Different Methods. *Chem. Phys. Lett.* **2009**, *472*, 96–98.

30 Ghosh, A.; Rao, K. V.; George, S. J.; Rao, C. N. R. Noncovalent Functionalization, Exfoliation, and Solubilization of Graphene in Water by Employing a Fluorescent Coronene Carboxylate. *Chem.—Eur. J.* **2010**, *16*, 2700–2704.

31 Ghosh, A.; Late, D. J.; Panchakarla, L. S.; Govindaraj, A.; Rao, C. N. R. NO_2 and Humidity Sensing Characteristics of Few-Layer Graphenes. *J. Exp. Nanosci.* **2009**, *4*, 313.

32 Hassan, H. M. A.; Abdelsayed, V.; Khder, A. E. R. S.; AbouZeid, K. M.; Terner, J.; El-Shall, M. S.; Al-Resayes, S. I.; El-Azhary, A. A. Microwave Synthesis of Graphene Sheets Supporting Metal Nanocrystals in Aqueous and Organic Media. *J. Mater. Chem* **2009**, *19*, 3832–3837.

33 Siamaki, A. R.; Khder, A. E. R. S.; Abdelsayed, V.; El-Shall, M. S.; Gupton, B. F. Microwave-Assisted Synthesis of Palladium Nanoparticles Supported on Graphene: A Highly Active and Recyclable Catalyst for Carbon-Carbon Cross-Coupling Reactions. *J. Catal.* **2011**, *279*, 1–11.

34 Moussa, S.; Abdelsayed, V.; Samy El-Shall, M. Laser Synthesis of Pt, Pd, CoO and Pd-CoO Nanoparticle Catalysts Supported on Graphene. *Chem. Phys. Lett.* **2011**, *510*, 179–184.

35 Moussa, S.; Siamaki, A. R.; Gupton, B. F.; El-Shall, M. S. Pd-Partially Reduced Graphene Oxide Catalysts (Pd/PRGO): Laser Synthesis of Pd Nanoparticles Supported on PRGO Nanosheets for Carbon-Carbon Cross Coupling Reactions. *ACS Catal.* **2012**, *2*, 145–154.

36 Subrahmanyam, K. S.; Manna, A. K.; Pati, S. K.; Rao, C. N. R. A Study of Graphene Decorated with Metal Nanoparticles. *Chem. Phys. Lett.* **2010**, *497*, 70–75.

37 Das, B.; Choudhury, B.; Gomathi, A.; Manna, A. K.; Pati, S. K.; Rao, C. N. R. Interaction of Inorganic Nanoparticles with Graphene. *Chem. Phys. Chem.* **2011**, *12*, 937–943.

38 Subrahmanyam, K. S.; Kumar, P.; Nag, A.; Rao, C. N. R. Blue Light Emitting Graphene-Based Materials and Their Use in Generating White Light. *Solid State Commun.* **2010**, *150*, 1774–1777.

39 Matte, H. S. S. R.; Subrahmanyam, K. S.; Venkata Rao, K.; George, S. J.; Rao, C. N. R. Quenching of Fluorescence of Aromatic Molecules by Graphene Due to Electron Transfer. *Chem. Phys. Lett.* **2011**, *506*, 260–264.

40 Wojcik, A.; Kamat, P. V. Reduced Graphene Oxide and Porphyrin. An Interactive Affair in 2-D. *ACS Nano* **2010**, *4*, 6697–6706.

41 Wang, X.; Li, X.; Zhang, L.; Yoon, Y.; Weber, P. K.; Wang, H.; Guo, J.; Dai, H. N-Doping of Graphene through Electrothermal Reactions with Ammonia. *Science* **2009**, *324*, 768–771.

42 Li, X. L.; Wang, H. L.; Robinson, J. T.; Sanchez, H.; Diankov, G.; Dai, H. J. Simultaneous Nitrogen Doping and Reduction of Graphene Oxide. *J. Am. Chem. Soc.* **2009**, *131*, 15939–15944.

43 Panchakarla, L. S.; Subrahmanyam, K. S.; Saha, S. K.; Govindaraj, A.; Krishnamurthy, H. R.; Waghmare, U. V.; Rao, C. N. R. Synthesis, Structure, and Properties of Boron- and Nitrogen-Doped Graphene. *Adv. Mater.* **2009**, *21*, 4726–4730.

44 Gopalakrishnan, K.; Joshi, H. M.; Kumar, P.; Panchakarla, L. S.; Rao, C. N. R. Selectivity in the Photocatalytic Properties of the Composites of TiO_2 Nanoparticles with B- and N-Doped Graphenes. *Chem. Phys. Lett.* **2011**, *511*, 304–308.

45 Elias, D. C.; Nair, R. R.; Mohiuddin, T. M. G.; Morozov, S. V.; Blake, P.; Halsall, M. P.; Ferrari, A. C.; Boukhvalov, D. W.; Katsnelson, M. I.; Geim, A. K.; Novoselov, K. S. Control of Graphene's Properties by Reversible Hydrogenation: Evidence for Graphane. *Science* **2009**, *323*, 610–613.

46 Zheng, L.; Li, Z.; Bourdo, S.; Watanabe, F.; Ryerson, C. C.; Biris, A. S. Catalytic Hydrogenation of Graphene Films. *Chem. Commun.* **2010**, *47*, 1213–1215.

47 Subrahmanyam, K. S.; Kumar, P.; Maitra, U.; Govindaraj, A.; Hembram, K.; Waghmare, U. V.; Rao, C. N. R. Chemical Storage of Hydrogen in Few-Layer Graphene. *Proc. Natl. Acad. Sci. U.S.A.* **2011**, *108*, 2674–2677.

48 Gopalakrishnan, K.; Subrahmanyam, K. S.; Kumar, P.; Govindaraj, A.; Rao, C. N. R. Reversible Chemical Storage of Halogens in Few-Layer Graphene. *RSC Adv.* **2012**, *2*, 1605–1608.

49 Yazyev, O. V.; Helm, L. Defect-Induced Magnetism in Graphene. *Phys. Rev. B* **2007**, *75*, No. 125408.

50 Bhowmick, S.; Shenoy, V. B. Edge State Magnetism of Single Layer Graphene Nanostructures. *J. Chem. Phys.* **2008**, *128*, No. 244717.

51 Wang, Y.; Huang, Y.; Song, Y.; Zhang, X. Y.; Ma, Y. F.; Liang, J. J.; Chen, Y. S. Room-Temperature Ferromagnetism of Graphene. *Nano Lett.* **2009**, *9*, 220–224.

52 Matte, H. S. S. R.; Subrahmanyam, K. S.; Rao, C. N. R. Novel Magnetic Properties of Graphene: Presence of Both Ferromagnetic and Antiferromagnetic Features and Other Aspects. *J. Phys. Chem. C* **2009**, *113*, 9982–9985.

53 Rao, C. N. R.; Matte, H. S. S. R.; Subrahmanyam, K. S.; Maitra, U. Unusual Magnetic Properties of Graphene and Related Materials. *Chem. Sci.* **2012**, *3*, 45–52.

54 Wu, Z.-S.; Pei, S.; Ren, W.; Tang, D.; Gao, L.; Liu, B.; Li, F.; Liu, C.; Cheng, H.-M. Field Emission of Single-Layer Graphene Films Prepared by Electrophoretic Deposition. *Adv. Mater.* **2009**, *21*, 1756–1760.

55 Palnitkar, U. A.; Kashid, R. V.; More, M. A.; Joag, D. S.; Panchakarla, L. S.; Rao, C. N. R. Remarkably Low Turn-on Field Emission in Undoped, Nitrogen-Doped, And Boron-Doped Graphene. *Appl. Phys. Lett.* **2010**, *97*, 063102.

56 Ye, D.; Moussa, S.; Ferguson, J. D.; Baski, A. A.; El-Shall, M. S. Highly Efficient Electron Field Emission from Graphene Oxide Sheets Supported by Nickel Nanotip Arrays. *Nano Lett.* **2012**, *12*, 1265–1268.

57 Late, D. J.; Ghosh, A.; Subrahmanyam, K. S.; Panchakarla, L. S.; Krupanidhi, S. B.; Rao, C. N. R. Characteristics of Field-Effect Transistors Based on Undoped and B- and N-Doped Few-Layer Graphenes. *Solid State Commun.* **2010**, *150*, 734–738.

58 Xia, F.; Mueller, T.; Lin, Y.-m.; Valdes-Garcia, A.; Avouris, P. Ultrafast Graphene Photodetector. *Nat. Nanotechnol.* **2009**, *4*, 839–843.

59 Chitara, B.; Panchakarla, L. S.; Krupanidhi, S. B.; Rao, C. N. R. Infrared Photodetectors Based on Reduced Graphene Oxide and Graphene Nanoribbons. *Adv. Mater.* **2011**, *23*, 5419–5424.

60 Lee, C.; Kim, J. Y.; Bae, S.; Kim, K. S.; Hong, B. H.; Choi, E. J. Optical Response of Large Scale Single Layer Graphene. *Appl. Phys. Lett.* **2011**, *98*, No. 071905.

61 Chitara, B.; Krupanidhi, S. B.; Rao, C. N. R. Solution Processed Reduced Graphene Oxide Ultraviolet Detector. *Appl. Phys. Lett.* **2011**, *99*, No. 113114.

62 Ramanathan, T.; Abdala, A. A.; Stankovich, S.; Dikin, D. A.; Herrera Alonso, M.; Piner, R. D.; Adamson, D. H.; Schniepp, H. C.; ChenX; Ruoff, R. S.; Nguyen, S. T.; Aksay, I. A.; Prud'Homme, R. K.; Brinson, L. C. Functionalized Graphene Sheets for Polymer Nanocomposites. *Nat. Nanotechnol.* **2008**, *3*, 327–331.

63 Prasad, K. E.; Das, B.; Maitra, U.; Ramamurty, U.; Rao, C. N. R. Extraordinary Synergy in the Mechanical Properties of Polymer Matrix Composites Reinforced with 2 Nanocarbons. *Proc. Natl. Acad. Sci. U.S.A.* **2009**, *106*, 13186–13189.

64 Tenne, R. Inorganic Nanotubes and Fullerene-Like Nanoparticles. *Nat. Nanotechnol.* **2006**, *1*, 103–111.

65 Coleman, J. N.; Lotya, M.; O'Neill, A.; Bergin, S. D.; King, P. J.; Khan, U.; Young, K.; Gaucher, A.; De, S.; Smith, R. J.; Shvets, I. V.; Arora, S. K.; Stanton, G.; Kim, H.-Y.; Lee, K.; Kim, G. T.; Duesberg, G. S.; Hallam, T.; Boland, J. J.; Wang, J. J.; Donegan, J. F.; Grunlan, J. C.; Moriarty, G.; Shmeliov, A.; Nicholls, R. J.; Perkins, J. M.; Grieveson, E. M.; Theuwissen, K.; McComb, D. W.; Nellist, P. D.; Nicolosi, V. Two-Dimensional Nanosheets Produced by Liquid Exfoliation of Layered Materials. *Science* **2011**, *331*, 568–571.

66 Matte, H. S. S. R.; Gomathi, A.; Manna, A. K.; Late, D. J.; Datta, R.; Pati, S. K.; Rao, C. N. R. MoS_2 and WS_2 Analogues of Graphene. *Angew. Chem., Int. Ed.* **2010**, *49*, 4059–4062.

67 Matte, H. S. S. R.; Plowman, B.; Datta, R.; Rao, C. N. R. Graphene Analogues of Layered Metal Selenides. *Dalton Trans.* **2011**, *40*, 10322–10325.

68 Nag, A.; Raidongia, K.; Hembram, K. P. S. S.; Datta, R.; Waghmare, U. V.; Rao, C. N. R. Graphene Analogues of BN: Novel Synthesis and Properties. *ACS Nano* **2010**, *4*, 1539–1544.

69 Matte, H. S. S. R.; Chitara, B.; Maitra, U.; Sharmila, N. S.; Krupanidhi, S. B.; Waghmare, U. V.; Rao, C. N. R. Superior Infrared Detection Properties of Few-layer $MoSe_2$. *ACS Nano.* **2012**, submitted for publication.

70 Kiran, M. S. R. N.; Raidongia, K.; Ramamurty, U.; Rao, C. N. R. Improved Mechanical Properties of Polymer Nanocomposites Incorporating Graphene-Like BN: Dependence on the Number of BN Layers. *Scr. Mater.* **2010**, *64*, 592–595.

71 Vivekchand, S. R. C.; Rout, C. S.; Subrahmanyam, K. S.; Govindaraj, A.; Rao, C. N. R. Graphene-Based Electrochemical Supercapacitors. *J. Chem. Sci.* **2008**, *120*, 9–13.